NIH Public Access
Author Manuscript
J Neurosci Methods. Author manuscript; available in PMC 2012 April 30.

Published in final edited form as:
J Neurosci Methods. 2011 April 30; 197(2): 238–248. doi:10.1016/j.jneumeth.2011.02.026.

Comparison of the efficacy of four viral vectors for transducing hypothalamic magnocellular neurosecretory neurons in the rat supraoptic nucleus

Faye C Doherty[a], **Jerome B Schaack**[b], and **Celia D Sladek**[a,*]

Faye C Doherty: Faye.Doherty@ucdenver.edu; Jerome B Schaack: Jerry.Schaack@ucdenver.edu

[a] Physiology and Biophysics Department, University of Colorado, School of Medicine, Aurora, CO, USA

[b] Microbiology Department, University of Colorado, School of Medicine, Aurora, CO, USA

1. Introduction

Magnocellular neurosecretory cells (MNCs), located in the paraventricular (PVN) and supraoptic (SON) nuclei of the hypothalamus, are neurons which produce vasopressin (AVP) and oxytocin (OT) and release them into the blood stream via exocytosis from axon terminals in the neurohypophysis (Bourque et al., 1994; Swanson and Sawchenko, 1983). AVP is necessary for homeostatic maintenance of both extracellular fluid (ECF) volume, which is necessary for normal cardiovascular function, and ECF osmolality, which is critical for neuronal excitability. It is an anti-diuretic agent and causes vasoconstriction (Sladek, 2000). During dehydration, AVP synthesis and release increase dramatically, and biosynthesis, neurotransmitter release, morphology and electrical properties of MNCs in the SON are altered to facilitate this increase. These changes are reversed by rehydration, making the hypothalamo-neurohypophyseal system (HNS) a good system for studying plasticity, neurotransmitter signaling and gene regulation, as well as physiology (Sharman et al., 2004).

Accurate regulation of AVP secretion is critical for human health. Insufficient secretion of AVP, causes dehydration (Ghirardello et al., 2007) and hemorhagic shock (Rajani et al., 2009). Excessive secretion of AVP causes hyponatraemia which leads to symptoms such as headache, nausea, vomiting, and confusion, and can be lethal (Sherlock and Thompson, 2010). Inappropriate AVP secretion is a common complication of congestive heart failure (Rosner, 2009).

Though the physiology of the HNS has been extensively studied, there are many aspects of its function and regulation that remain poorly understood. The ability to modulate gene expression in this system *in vivo* is essential for elucidating the interactions between gene regulation and physiology. Transgenic mice are available for studying many genes of interest, but functional compensation from related genes is not uncommon in knockout

© 2011 Elsevier B.V. All rights reserved.

*Corresponding author: Postal address: University of Colorado, School of Medicine, Department of Physiology and Biophysics, RC-1 North Tower, P18-7127, Mail Stop 8307, Aurora, CO 80045, Phone number: 303-724-4526, Fax number: 303-724-4501, Celia.Sladek@ucdenver.edu.

Publisher's Disclaimer: This is a PDF file of an unedited manuscript that has been accepted for publication. As a service to our customers we are providing this early version of the manuscript. The manuscript will undergo copyediting, typesetting, and review of the resulting proof before it is published in its final citable form. Please note that during the production process errors may be discovered which could affect the content, and all legal disclaimers that apply to the journal pertain.

NIH-PA Author Manuscript
NIH-PA Author Manuscript
NIH-PA Author Manuscript

NIH-PA Author Manuscript

NIH-PA Author Manuscript

NIH-PA Author Manuscript

models and complicates phenotype interpretation. Furthermore, the majority of physiological and functional studies of the HNS have been conducted in rats, but transgenic rats are not widely available.

In contrast to knockout models, viral vectors can be targeted to specific tissues or brain nuclei, injected at any desired developmental stage and provide prolonged expression of the cloned construct. Plus, transduced cells can be visualized using marker transgenes, such as lacZ or GFP. Combined with their innate ability to transport nucleic acids into eukaryotic cells, this specificity makes viral vectors ideal for delivering transgenes or gene silencing constructs (such as antisense or RNAi) into experimentally relevant cell populations. Furthermore, localized use of viral vectors in adult animals allows for the study of differing roles of a gene in distinct organs or brain regions. Plus, vector experiments can be translated from one model animal to another relatively easily since most vectors are similarly effective in a wide variety of mammals; this is particularly useful in animals where germline manipulation is not feasible, such as non-human primates.

Vector mediated delivery is a powerful method for studying gene function, but achieving efficient, precise transduction *in vivo* presents many challenges, particularly in the CNS. The goal is to transduce a high percentage of target cells, in this case MNCs, without significant involvement of tissue beyond the area of interest or transduction of other cell types, such as glia. To achieve this, an appropriate viral vector for a particular cell population needs to be identified, and titer, volume and time course of the injection require optimization for maximal transduction of cells in the target area and minimal transduction of surrounding tissue.

Since MNCs are located in both the SON and the PVN, either nucleus can be targeted for studying gene function in the HNS. The SON is scientifically advantageous because its neuronal population is homogenous (MNCs are the only neurons). However, it is also more challenging to specifically transduce the SON because of its oblong shape; it is approximately 1.5mm long, but has a diameter of only about 400μm at its widest point. The magnocellular region of the PVN, on the other hand, is methodologically advantageous because it is smaller and roughly spherical. With a diameter of less than 300μm, it is much easier to target all PVN MNCs with a single injection. The disadvantage of targeting the PVN is that its neuronal population is heterogeneous, and many genes expressed in MNCs are also expressed in surrounding parvocellular neurons. Thus, any observed effects of gene expression modulation cannot be conclusively attributed to MNCs.

Viral vectors have been used successfully to reverse diabetes insipidus in Brattleboro rats [adenovirus: (Geddes et al., 1997); equine infectious anemia virus (EIAV), a lentivirus: (Bienemann et al., 2003); AAV2: (Ideno et al., 2003)], a strain in which a naturally-occurring mutation in the AVP gene prevents its synthesis (Ivell et al., 1990; Schmale and Richter, 1984). Reversal of diabetes insipidus required relatively low transduction efficiency and minimal AVP expression; the lentivirus (EIAV) transduced only about 50% of SON neurons (Bienemann et al., 2003), and AAV2 increased pituitary AVP content only up to 10% of normal (Ideno et al., 2003). In contrast, studies on subtle genetic effects, particularly downregulation of homeostatically regulated genes, require more efficient transduction. The aim of the studies presented here was to identify the most effective viral vector and delivery technique for transducing MNCs of the HNS.

2. Materials and methods

Four viral vectors were evaluated for their ability to transduce MNC neurons when stereotaxically injected into the rat hypothalamus. In each case, GFP was used as a reporter

NIH-PA Author Manuscript

NIH-PA Author Manuscript

NIH-PA Author Manuscript

transgene, and GFP immunohistochemistry was used to visualize transduced cells in frozen brain sections.

2.1. Animals

Adult male Sprague-Dawley rats (280–370g; Charles River) were housed at an ambient temperature of 21°C with a 12:12 hour light-dark cycle. Food was provided ad libidum, as was water, except for 24 hours before and 4–7 days after surgery, when a solution of 2.0mg/ml acetaminophen in 1% sucrose was provided instead. All protocols used were performed in accordance with the National Institutes of Health Guidelines for the Care and Use of Laboratory Animals and were approved by the Institutional Animal Care and Use Committee of the University of Colorado Denver.

2.2. Stereotaxic injection

Rats were anesthetized with Avertin (0.4mg 2,2,2 tribromoethanol/g BW, i.p., prepared in saline, Sigma Aldrich). Using a 10μl Hamilton syringe, vector solution was stereotaxically injected just above the SON or PVN either uni- or bilaterally. Coordinates (detailed in Table 1) were measured from bregma after leveling the skull between bregma and lambda. A 30G stainless steel cannula was inserted into the brain through a small hole drilled through the top of the skull. Adenoviral and lentiviral vector solutions were injected at a rate of 0.1μl/min. Small volumes of adenovirus were injected in order the limit the volume of surrounding tissue that was affected. This was not possible with the lentiviral vector due to the fact that it cannot be as highly concentrated as adenoviral and AAV vectors. The AAV vectors were injected using a convection-enhanced delivery protocol (developed by Dr. Harold Gainer, personal communication), which was designed to maximize AAV transduction throughout the length of the SON by using a larger volume of injectate (2.5μl) injected more rapidly (0.25μl/min). The injector was left in place for 5 minutes before and 10 minutes after the injection to minimize diffusion up the cannula track. Table 1 contains vector specific injection details.

2.3. Vectors

The adenoviral vector (Ad-GFP) was serotype 5, replication defective, deleted for E1A, E1B and E3, with a transgene cassette containing the CMV major immediate early promoter driving GFP expression and the SV40 bidirectional poly A site. Viral stock was purified by CsCl step and isopycnic gradient centrifugation. The vector was then dialyzed into 50% glycerol as a cryoprotective in a buffer (10mM Tris, 10mM His, 75mM NaCl, 0.5% v/v EtOH, 1mM MgCl, 0.1mM EDTA, and 50% v/v glycerol) optimized for the maintenance of adenoviral viability [(Evans et al., 2004)* but with 50% glycerol substituted for 5% sucrose as cryoprotectant], and diluted in PBS immediately prior to the injection. The concentration of the highly purified virus was determined spectrophotometrically, with 1 OD260 equivalent to 10^{12} particles/ml and a particle:pfu ratio of 100:1. The spectrophotometric method was used because it is consistent among highly purified adenoviral stocks, whereas plaque sizes vary among different adenoviral vectors (Schaack et al., 2011).

The lentiviral human immunodeficiency virus (HIV) vector was VSVG pseudotyped and encoded GFP driven by the CMV major immediate early promoter. HEK293FT cells were transfected with plasmids containing the HIV proviral vector encoding GFP, the helper plasmid encoding Gag, Pol, rev, and tat, and the plasmid encoding VSVG. Twelve hours later, the cells were fed fresh medium. Forty-eight hours after transfection, the medium was collected. Cell debris was removed by low-speed centrifugation. The supernatant was then centrifuged at 60,000×g for 90 minutes to pellet the HIV vector. The vector was resuspended by triteration in PBS, passed through a 0.45μm filter, and centrifuged under sterile conditions at 60,000×g for 90 minutes. The pelleted virus was resuspended by

NIH-PA Author Manuscript

NIH-PA Author Manuscript

NIH-PA Author Manuscript

triteration in a 200μl of PBS and frozen at −80°C in 10μl aliquots. The virus was titered in HEK293 cells using GFP fluorescence and counted using a fluorescent microscope.

The AAV2 construct (rAVE, GeneDetect; provided by Alan Kim Johnson) encoded GFP driven by a CAG promoter and enhanced by a woodchuck hepatitis virus post transcriptional regulatory element (WPRE). The CAG promoter is a combination of the chicken B-actin promoter and the CMV early enhancer element (Xu et al., 2001a). Viral particles were affinity purified on columns using immobilised heparan sulfate proteoglycan (Clark et al., 1999; Zolotukhin et al., 1999). The vector was suspended in PBS with 1mM $MgSO_4$ added to prevent clumping of vector particles. The vector was titrated using RT-PCR with primers designed against the WPRE sequence.

The AAV5 vector (AAV2/5-GFP, Vector Biolabs) contained inverted terminal repeats (ITR) from serotype 2 and was pseudotyped with capsid proteins from serotype 5. It encoded a CMV-EGFP-poly(A) transgene cassette. AAV5 stock was purified using a CsCl gradient, and viral titer (GC) was quantified using qPCR. The vector was suspended in PBS with 5% glycerol as a cryoprotective agent to enable storage at −80ºC.

A different range of timepoints was used for each vector based on previous reports and their differing expression latencies. A variety of timepoints was used for each vector in an effort to optimize the transduction protocols, with the exception of the AAV2. The four week timepoint was chosen for this vector based on the results with the AAV5 vector.

2.4. Tissue preparation

Animals were sacrificed using transcardial perfusion with physiological saline, followed by 4% paraformaldehyde with or without 2–2.5% acrolein. After removal, brains were placed in a 30% sucrose solution at 4°C until they sank (~48 hours). 30μm thick brain sections were sliced on a cryostat and stored at −20°C in antifreeze solution (30% sucrose, 30% ethylene glycol, 1% polyvinylpyrrolidone in 0.1M PBS) until immunostained.

2.5. Immunohistochemistry

Sections were removed from the antifreeze and: 1) thoroughly rinsed, 2) treated with 1% sodium borohydride for 20 minutes (only if acrolein fixed), 3) rinsed, and 4) blocked with 1% BSA, 3% horse serum, and 1% hydrogen peroxide for 1 hour before incubation in rabbit polyclonal anti-GFP (1 hour 37°C, 36–72 hours 4°C; 1:200k, ab290, Abcam). Slices were then: 1) thoroughly rinsed, 2) incubated in secondary antibody (biotinylated anti-rabbit, 1:600, Vector Laboratories) for 1 hour, 3) rinsed, 4) incubated in avidin-biotin complex (Vector Elite Kit; Vector Laboratories) for 1 hour and 5) rinsed before visualization of primary antibody with either a conventional (brown reaction product) or nickel-enhanced (dark purple reaction product) immunoperoxidase method. The slices were then rinsed and mounted on poly-L-lysine coated slides. After drying overnight, the slides were ethanol dehydrated, xylene treated, and coverslipped with Krystalon (Harleco, EM Science).

For ERβ/GFP double labeling, the ERβ antibody was a rabbit polyclonal raised against aa 468–485 of the C-terminus of the mouse ERβ protein [Zymed, Z8P (Shughrue and Merchenthaler, 2001)] and was used at a 1:1500 dilution.

The absence of staining in brain regions away from the viral injections (Figs. 1a,2a,4a,5g,6c) and in unmanipulated rat brains (data not shown) confirms the specificity of the anti-GFP antibody (ab290); the point mutation difference between GFP to EGFP (F64L) is unlikely to affect antibody sensitivity or specificity since it is a polyclonal antibody raised against the full length protein. This antibody has been used extensively, including in rodent brains (Faulkner et al., 2008; Ma et al., 2008).

NIH-PA Author Manuscript

NIH-PA Author Manuscript

NIH-PA Author Manuscript

2.6. Imaging

All images were acquired on an Olympus Provis AX70 microscope using a Prior Proscan II camera and Microsuite Biological Suite software. The images shown are extended focal images (EFI), in which the in-focus parts of a sequence of aligned images are combined to produce a single image with an increased depth of field. EFI were created using 5–7 z-stack images spanning 12–20μm, taken with either a 10×, 20× or 40× objective.

2.7. Cell counts

For each brain, eight stained sections of 30μm spaced 210μm apart (every eighth section) were imaged and GFP-positive cells were counted. Using the cell counter plugin in ImageJ (NIH's open source image analysis program), each GFP-positive soma was marked, and the software counted the number of marks on the image. The cell counts were totaled for each injected nucleus; in bilaterally injected brains, the two SONs were treated as separate data points (one data point per injection). Analysis of variance (one-way ANOVA) was used to determine that the groups were not all equivalent, and Student's t-tests (two-tailed, unpaired, unequal variance) were used post-hoc to compare cell counts between time points (two versus three weeks, two versus four weeks, and three versus four weeks). $p<0.05$ was used to determine statistical significance.

3. Results

3.1. Adenovirus

Injection of the adenoviral vector encoding GFP (Ad-GFP) into the SON (6.66×10^7 pfu in 0.6μl) resulted in sparse GFP expression in both glia and neurons, in and around the SON four days later (Fig. 1a). Increasing the titer and volume of the injectate to 1.11×10^9 pfu in 1.0μl resulted in a dramatic increase in the number of GFP positive glia and neurons (Fig. 1b). Prominent glial staining was evident in the SON, surrounding hypothalamic tissue (particularly along the cannula track), the astrocytic glial lamina ventral to the SON (VGL) and the optic chiasm. The high density of glial GFP staining and the difficulty visualizing cell bodies made accurate quantification of the number of transduced neurons difficult. However, the presence of transduced MNCs is confirmed by the presence of GFP positive fibers in the hypothalamo-neurohypophyseal (HN) tract (Fig. 1c) and in the internal zone (IZ) of the median eminence (ME; Fig. 1d), since axons extending from MNC soma in the SON to the neural lobe of the pituitary follow this path. Stained fibers in the external zone (EZ) of the ME indicate that the scattered neurons in the lateral hypothalamus which were transduced include some that project to the hypophyseal portal veins in the basal hypothalamus. Tanycytes and their fibers, as well as other ependymal cells lining the third ventricle, are also visible above the ME (Fig. 1c). The exposure of these cells to Ad-GFP is most likely due to the injector passing through the lateral ventricle.

Ad-GFP was also tested in the PVN. Seven days after Ad-GFP injection (1.00×10^7pfu in 0.5μl), the PVN showed a transduction pattern similar to that seen with the higher titer in the SON at four days (Fig. 2a); GFP expression was widespread, but high expression in overlapping cells of various types prevented convincing visualization of GFP positive neurons. Stained fibers in both the internal and external zones of the ME (Fig. 2b) indicate transduction of both magnocellular and parvocellular PVN neurons. Axons from PVN MNCs pass through the HN tract and the internal zone en route to the neural lobe of the pituitary, while parvocellular PVN neurons regulate anterior pituitary function through axons that terminate on the portal vessels in the external zone of the ME.

The time course of GFP expression was also similar between the SON and the PVN. GFP expression was robust four days (Fig. 1a,b,c) and seven days (Fig. 2a,b) post-injection. After

NIH-PA Author Manuscript

NIH-PA Author Manuscript

NIH-PA Author Manuscript

two weeks, however, GFP expression was reduced dramatically in the SON (Fig. 3a; 1.11×10^8 pfu in 1.0μl) and somewhat in the PVN (Fig. 3c; 1.00×10^7 pfu in 0.5μl). After four weeks, GFP expression in both nuclei persisted only in a few scattered cells (Fig. 3b,d). Reduction of transgene expression this soon after adenoviral injection was contradictory to expectations based on previous reports (Geddes et al., 1996; Geddes et al., 1997; Sinnayah et al., 2002; Sinnayah et al., 2004), but indicates that this vector may be more suitable for short term studies, rather than chronic ones.

3.2. Lentivirus (HIV)

Injection of a lentiviral vector encoding GFP (HIV-GFP; 5.0×10^5 TU in 1.0μl) into the SON resulted in only a few GFP positive SON MNCs four days post-injection (Fig. 4a). After eight days, the number of GFP positive MNCs was noticeably increased (Fig. 4b), but they remained localized to a small area surrounding the injection site. GFP positive glia were also prevalent in the SON at both time points (Fig. 4a,b), and were particularly numerous along the cannula track through the hypothalamus. Since a maximally concentrated stock solution was used for these injections, increasing the viral concentration of the injectate was not possible; instead, an increased volume (2.5μl) was injected in an attempt to increase the number of transduced MNCs. This resulted in visibly more GFP positive MNCs at the eight day time point, but the number of transduced glia was also dramatically increased (Fig. 4c). The GFP positive glia were large cells, with their processes covering an area of about 50μm in diameter, and were quite dense near the cannula track (Fig. 4d). Transduced glia all exhibited a similar morphology of extremely densely ramified fine processes; this spongiform morphology is characteristic of mature protoplasmic astrocytes (Bushong et al., 2004). This was most clearly seen in isolated cells farther from the cannula track (Fig. 4e).

3.3. AAV2

Using a convection enhanced delivery protocol (2.5μl at 0.25 μl/min) to inject the serotype 2 AAV vector resulted in diffusion of the construct throughout the anterior to posterior extent of the SON, as demonstrated by the extensive transduction of neurons in the anterior (Fig. 5a), mid (Fig. 5b) and posterior (Fig. 5c) SON, as well as surrounding hypothalamic tissue (Fig. 5a–d).

GFP staining was much darker and more widespread in AAV2 injected brains relative to that seen with any other construct. One possible explanation is that the WPRE element in the AAV2 construct enhanced GFP expression; it is a post transcriptional enhancer that facilitates cytoplasmic accumulation and translation of mRNA (Loeb et al., 1999). The expression enhancing properties of the WPRE element have been confirmed in rat brain, with 4- to 9- fold increases in luciferase expression in various brain regions (Xu et al., 2001b) and an 11-fold increase in GFP expression in the hippocampus (Klein et al., 2002). It is also possible that the CAG promoter for GFP in the AAV2 construct was stronger than the CMV promoter in the other three constructs. The CAG promoter is a combination of the cytomegalovirus early enhancer element and chicken β-actin promoter and was designed to drive high levels of gene expression. It has previously been shown in liver that in an AAV vector the CAG promoter drives much higher levels of gene expression than a CMV promoter (Xu et al., 2001a). It has also been shown that AAV8-CAG-GFP results in brighter GFP fluorescence in hippocampus than AAV8-CMV-GFP (Klein et al., 2007).

The high GFP expression is particularly striking in neurites, which were extremely dense throughout the ipsilateral hypothalamus, leading to dark staining of the tissue surrounding the SON (Fig. 5a–d). Viewing the entire hypothalamus at low power demonstrates that the dark staining is restricted to the injected side of the hypothalamus (Fig. 5d). At high magnification, individual neurons and the web of neurites can be clearly seen (Fig. 5f). In

NIH-PA Author Manuscript

NIH-PA Author Manuscript

NIH-PA Author Manuscript

the contralateral hypothalamus, stained neurites are still prevalent, but much less dense than on the injected side, and GFP positive cell bodies are completely absent (Fig. 5g). The contralateral SON also shows no GFP positive cell bodies, though fibers are present in the surrounding tissue (Fig. 5h).

The high density of stained neurons and fibers prevented the accurate counting of GFP positive MNC somas, but very high staining density in the SON and fibers in the internal zone of the ME (Fig. 5e) indicate efficient transduction of MNCs. Though dense staining in the SON makes it inconclusive whether or not there are transduced glia, GFP positive cells in the surrounding tissue have exclusively neuronal morphologies. Dark staining of the ventral glial lamina ventra-lateral to the SON most likely reflects the high density of MNC dendrites in this region, rather than the astrocytic transduction seen with the adenovirus (Fig. 1).

3.4. AAV5

Injection of the AAV5 vector into the SON using the convection enhanced protocol resulted in transduction of a reasonable percent of SON MNCs three weeks post-injection. GFP positive cells were distributed throughout the nucleus (Fig. 6a: anterior SON; 6c mid SON; 6e posterior SON), and demonstrated somewhat selective transduction of the SON, with fewer neurons and no glia transduced in the surrounding tissue (Fig. 6a,c,e). Four weeks post-injection, the selectivity and extent of MNC transduction remained evident, and the number of GFP positive MNCs was dramatically increased (Fig. 6b: anterior SON; 6d mid SON; 6f posterior SON). Due to GFP expression being primarily restricted to cell bodies, MNCs could be clearly visualized, and AAV5 transduction was conclusively observed to be restricted to neurons. GFP expression was undetectable in most MNC neurites, and consequently, GFP expression in the ME was minimal after either three (Fig. 6f) or four weeks (Fig. 6g), despite efficient transduction of MNCs.

Since individual cells were easily distinguished, GFP positive MNCs were counted two, three and four weeks post-injection (Fig. 7). Five injections (n=5) from three rats (two injected bilaterally, one unilaterally) were analyzed for each time point. For each injection, cells were counted on eight equally-spaced 30μm sections (every eighth section) spanning the entire length of the SON. The number of SON neurons expressing detectible levels of GFP was equivalent after two or three weeks, but doubled between three and four weeks. This increase was statistically significant (one-way ANOVA, $p=0.003$; t-test two versus four weeks, $p=0.010$; t-test three versus four weeks, $p=0.015$). Based on previous cell counts in the rat SON (Rhodes et al., 1981), GFP expression was evident in 30–50% of MNCs in the targeted nuclei four weeks post-injection. Rhodes et al. calculated that each SON contains about 4600 MNCs. Since we counted cells in every eighth slice, we would expect to count $4600 \div 8 = 575$ cells, if every neuron were transduced. By this approximation, our average (at four weeks) of 233 GFP positive MNCs per nucleus indicates transduction of about 40% of SON MNCs. The most successful injections (up to 322 cells counted) resulted in the transduction of more than 50% of SON MNCs. Thus, a respectable percent of MNCs were transduced by AAV5.

4. Discussion

In this study we evaluated four viral vectors (adenovirus, HIV, AAV2 and AAV5) for their ability to transduce MNC neurons in the rat hypothalamus, and found that all four were capable of driving transgene expression in SON MNCs. Each vector has advantages and disadvantages, however, and the usefulness of each depends on the experimental design and end points analyzed. Table 2 summarizes many of the differences among the three types of vectors tested.

NIH-PA Author Manuscript

NIH-PA Author Manuscript

NIH-PA Author Manuscript

A particularly important factor in selection of a viral vector for a given application is knowing what cell types it is able to transduce, often referred to as the cell tropism of a virus or vector. The two AAV vectors demonstrated efficient neuronal transduction with minimal or no glial transduction. On the other hand, Ad-GFP and HIV-GFP did not show this exclusivity. Consistent with previous studies using adenoviral vectors in the HNS and elsewhere in the brain (Puntel et al., 2010; Vasquez et al., 2001), Ad-GFP had a broad cell tropism in the hypothalamus, making cell bodies difficult to visualize, and minimal expression in ME fibers suggested only moderate transduction efficiency of MNCs. Though glial transduction could be problematic for some studies, it could be advantageous for studying gene function in glia since there are currently no vectors with glial tropism that do not transduce neurons; glial-specific transgene expression has only been achieved using specific promoters, such as glial fibrillary acidic protein (Howarth et al., 2009).

The lentiviral vector, HIV-GFP, had not been previously evaluated in the SON, and transduced fewer MNCs than any of the other constructs, but this is likely due to the titer of the injectate being two to four orders of magnitude lower than for the other vectors. HIV-GFP transduction of glia was prevalent, but appeared restricted to protoplasmic astrocytes close to the injection site and cannula track. Our vector also showed a much lower transduction efficiency than EIAV, the lentiviral vector used to restore AVP to the SON in Brattleboro rats (Bienemann et al., 2003), despite both vectors being pseudotyped with VSVG. Unlike the transduction pattern we observed with HIV-GFP, EIAV transduced almost exclusively neurons (Bienemann et al., 2003). Lentiviral vectors injected in the preoptic area of rats also showed predominantly neuronal transduction (Heger et al., 2007), though transduction efficiency was similar to what we observed with the HIV-GFP. One explanation for the fact that we observed higher glial transduction than is usually reported with lentiviral vectors in the hypothalamus is that we looked at an earlier time point than those used in other studies. Furthermore, some previous studies have shown efficient lentiviral transduction of glia, including astrocytes in primary culture (Li et al., 2010), astrocytes and microglia in spinal cord (Meunier and Pohl, 2009), and glia in the rostral midbrain (Blits et al., 2010). Though the number of transduced MNCs we observed with HIV-GFP was too low to have physiological or downstream effects from genetic manipulation, it could be useful in studies comparing transduced and non-transduced cells side by side.

A key factor in whether a given vector is effective for achieving transgene expression in a given cell type is whether that cell type expresses the appropriate receptor. The HIV-GFP vector used here was pseudotyped with the VSVG envelope glycoprotein, which confers a broad tropism and increases vector particle stability (Escors and Breckpot, 2010), so it is not surprising that transduction in the hypothalamus is not restricted to neurons. While retroviral infection usually requires interaction between the viral envelope protein and specific receptors on the cell surface, VSVG interacts with phospholipids in the cell membrane to mediate fusion between the cell membrane and the viral envelope, enabling viral entry (Conti et al., 1988; Harrison, 2008; Mastromarino et al., 1987). The primary receptor used by adenoviral vectors is the coxsackie and adenovirus receptor (Bergelson et al., 1997). It is widely expressed on neurons and reactive astrocytes (Persson et al., 2007), but is present at much higher levels during development than in adults in both brain regions in which this has been investigated [cortex: (Ahn et al., 2008); olfactory bulb: (Venkatraman et al., 2005)].

The membrane receptors used by AAV vectors to gain entry into host cells is dependent on the capsid proteins, which are serotype specific. For AAV2, heparin sulfate proteoglycans serve as primary receptors mediating viral attachment to and infection of host cells (Summerford and Samulski, 1998), while fibroblast growth factor (FGF) receptor 1 and αVβ5 integrin can act as coreceptors (Qing et al., 1999; Summerford et al., 1999). Platelet

NIH-PA Author Manuscript

NIH-PA Author Manuscript

NIH-PA Author Manuscript

derived growth factor receptor alpha (PDGFRα) has been shown to determine AAV5 tropism *in vitro* (Pasquale et al., 2003). In the brain, however, PDGFRα is exclusively expressed in oligodendrocyte progenitor cells, which were not transduced by AAV5. In the dorsal root ganglion, AAV5 was particularly efficient at transducing peptidergic neurons [almost 90% efficiency; (Mason et al., 2010)]. In combination with the efficient transduction of MNCs, this suggests an AAV5 tropism for peptidergic neurons. However, the data are only suggestive and further investigation is needed.

Though adenoviral vectors were first tested in the brain almost 20 years ago (Akli et al., 1993; Davidson et al., 1993; Le Gal La Salle et al., 1993) and have been widely used for genetic manipulation in the CNS, they have the disadvantage of triggering inflammation in transduced tissue (Puntel et al., 2010). This response has been extensively studied (Descamps and Benihoud, 2009), and because of the blood brain barrier, is less pronounced in the CNS than in peripheral organs. AAV vectors are not considered to be inflammatory, but reactive astrocytes and activated microglia have been reported in response to AAV injections in the striatum (Reimsnider et al., 2007). Interestingly, this was only observed when transgenes were driven by a strong promoter, and no sham injected animals were included in the study.

Though AAV2 was the first serotype of AAV used as a gene delivery vector, and remains the most widely used, more than a dozen AAV serotypes have been identified, and many of them have been evaluated in the CNS (Blits et al., 2010; Cearley and Wolfe, 2007; de Backer et al., 2010; Mason et al., 2010; Pasquale et al., 2003; Reimsnider et al., 2007). In multiple studies, AAV5 has been shown to spread farther and transduce more neurons than AAV2 (Burger et al., 2004; Mason et al., 2010; Paterna et al., 2004). In our studies, however, both AAV5 and AAV2 transduced many SON MNCs. Since quantification of GFP positive MNCs was not feasible in AAV2 injected brains, it is not clear whether its transduction efficiency was lower than AAV5. Even so, AAV5 was the only vector to show a preference for neurons within the SON over those of the surrounding hypothalamus. No previous studies have been published using this serotype of AAV in the HNS, but our results suggest that it may be a particularly useful vector for gene expression manipulation in the SON. AAV2 also efficiently transduced SON MNCs, but showed extensive transduction of other hypothalamic neurons as well. Neither AAV vector demonstrated transduction of non-neuronal cell types, and both maintained widespread GFP expression levels one month post-injection.

Direct comparisons between the two AAV vectors are complicated by the fact that they drove vastly different levels of GFP expression. Using very strong promoters/enhancers to drive high gene expression, as in our AAV2 vector, would be useful for some applications, such as live cell imaging where brighter fluorescence is beneficial, or transduction with a functional gene of interest where a high level of ectopic or overexpression is desired. For visualization of a marker gene, however, moderate expression is sufficient and often preferable.

One potential disadvantage of AAV vectors is that they are quite small [18–26nm (Atchison et al., 1965)], and consequently cannot package long DNA sequences (not more than 5kb). Because of this, AAV is well suited for RNAi applications, but can be problematic for overexpression studies; some genes of interest are too large for these vectors, particularly if coexpression of a marker gene is desired.

The prolonged transgene expression we report with AAV is typical of these vectors; most studies do not observe a reduction in transgene expression even at the latest time point assessed [four weeks: (Burger et al., 2004); twelve weeks: (Mason et al., 2010); nine months

NIH-PA Author Manuscript

NIH-PA Author Manuscript

NIH-PA Author Manuscript

(Burger et al., 2004; Mason et al., 2010; Paterna et al., 2004)]. On the other hand, the long latency between injection and strong transgene expression of AAV5 can be disadvantageous. For all AAV serotypes, the rate limiting step in transgene expression is synthesis of the second strand of DNA, but in various studies AAV5 has been shown to take significantly longer than other serotypes to attain peak transgene expression (Blits et al., 2010; Mason et al., 2010; Reimsnider et al., 2007). Consistent with the literature, we observed delayed GFP expression with the AAV5 vector. The number of GFP positive MNCs doubled between three and four weeks post-injection, and it is possible that expression had not yet peaked, since this was the latest time point we investigated. This slow onset of expression is not ideal for acute experiments, but the sustained expression is advantageous for chronic studies.

5. Conclusion

Overall, the data presented here demonstrate that of the four viral vectors examined (adenovirus, lentivirus, AAV2 and AAV5), the serotype 5 AAV vector was the most effective. When stereotaxically injected just above the anterior SON of adult rats it transduced a high percentage of MNCs throughout the nucleus and transgene expression remained high for at least a month. AAV vectors are useful for expressing short coding or silencing sequences in cells, and the selectivity of AAV5 for MNCs and its ability to maintain prolonged gene expression make it a very promising vector for specific genetic manipulation localized to neurons in the SON. A detailed understanding of this system at the molecular level is central to developing appropriate and effective treatments for cardiovascular diseases. Localized and acute modulation of specific genes in this nucleus holds the potential to greatly increase our understanding of HNS function, and lead to identification of target genes that may be important throughout the nervous system.

Acknowledgments

We would like to thank Alan Kim Johnson for providing the AAV2 vector, Harold Gainer for sharing his convection-enhanced delivery protocol, and John Sladek for providing the imaging facilities. We would also like to thank Wanida Stevens for doing an excellent job managing and organizing the lab. This work was supported by the National Institutes of Health (RO1 NS027975).

References

Ahn J, Jee Y, Seo I, Yoon SY, Kim D, Kim YK, Lee H. Primary neurons become less susceptible to coxsackievirus B5 following maturation: The correlation with the decreased level of CAR expression on cell surface. Journal of Medical Virology. 2008; 80:434–40. [PubMed: 18205224]

Akli S, Caillaud C, Vigne E, Stratford-Perricaudet LD, Poenaru L, Perricaudet M, Kahn A, Peschanski MR. Transfer of a foreign gene into the brain using adenovirus vectors. Nat Genet. 1993; 3:224–8. [PubMed: 8485577]

Atchison RW, Casto BC, Hammon WM. Adenovirus-Associated Defective Virus Particles. Science. 1965; 149:754–5. [PubMed: 14325163]

Bergelson JM, Cunningham JA, Droguett G, Kurt-Jones EA, Krithivas A, Hong JS, Horwitz MS, Crowell RL, Finberg RW. Isolation of a Common Receptor for Coxsackie B Viruses and Adenoviruses 2 and 5. Science. 1997; 275:1320–3. [PubMed: 9036860]

Bienemann AS, Martin-Rendon E, Cosgrave AS, Glover CPJ, Wong L-F, Kingsman SM, Mitrophanous KA, Mazarakis ND, Uney JB. Long-term replacement of a mutated nonfunctional CNS gene: reversal of hypothalamic diabetes insipidus using an EIAV-based lentiviral vector expressing arginine vasopressin. Mol Ther. 2003; 7:588–96. [PubMed: 12718901]

Blits B, Derks S, Twisk J, Ehlert E, Prins J, Verhaagen J. Adeno-associated viral vector (AAV)-mediated gene transfer in the red nucleus of the adult rat brain: Comparative analysis of the

NIH-PA Author Manuscript

NIH-PA Author Manuscript

NIH-PA Author Manuscript

transduction properties of seven AAV serotypes and lentiviral vectors. Journal of Neuroscience Methods. 2010; 185:257–63. [PubMed: 19850079]

Bourque CW, Oliet SHR, Richard D. Osmoreceptors, Osmoreception, and Osmoregulation. Frontiers in Neuroendocrinology. 1994; 15:231–74. [PubMed: 7859914]

Burger C, Gorbatyuk OS, Velardo MJ, Peden CS, Williams P, Zolotukhin S, Reier PJ, Mandel RJ, Muzyczka N. Recombinant AAV Viral Vectors Pseudotyped with Viral Capsids from Serotypes 1, 2, and 5 Display Differential Efficiency and Cell Tropism after Delivery to Different Regions of the Central Nervous System. Mol Ther. 2004; 10:302–17. [PubMed: 15294177]

Bushong EA, Martone ME, Ellisman MH. Maturation of astrocyte morphology and the establishment of astrocyte domains during postnatal hippocampal development. International Journal of Developmental Neuroscience. 2004; 22:73–86. [PubMed: 15036382]

Cearley CN, Wolfe JH. A Single Injection of an Adeno-Associated Virus Vector into Nuclei with Divergent Connections Results in Widespread Vector Distribution in the Brain and Global Correction of a Neurogenetic Disease. J Neurosci. 2007; 27:9928–40. [PubMed: 17855607]

Clark KR, Liu X, McGrath JP, Johnson PR. Highly purified recombinant adeno-associated virus vectors are biologically active and free of detectable helper and wild-type viruses. Human Gene Therapy. 1999; 10:1031–9. [PubMed: 10223736]

Conti C, Mastromarino P, Ciuffarella M, Orsi N. Characterization of rat brain cellular components acting as receptors for vesicular stomatitis virus. Brief report. Arch Virol. 1988; 99:261–9. [PubMed: 2835950]

Davidson BL, Allen ED, Kozarsky KF, Wilson JM, Roessler BJ. A model system for in vivo gene transfer into the central nervous system using an adenoviral vector. Nat Genet. 1993; 3:219–23. [PubMed: 8387378]

de Backer MWA, Brans MAD, Luijendijk MC, Garner KM, Adan RAH. Optimization of Adeno-Associated Viral Vector-Mediated Gene Delivery to the Hypothalamus. Human Gene Therapy. 2010; 21:673–82. [PubMed: 20073991]

Descamps D, Benihoud K. Two key challenges for effective adenovirus-mediated liver gene therapy: innate immune responses and hepatocyte-specific transduction. Current Gene Therapy. 2009; 9:115–27. [PubMed: 19355869]

Escors D, Breckpot K. Lentiviral Vectors in Gene Therapy: Their Current Status and Future Potential. Archivum Immunologiae et Therapiae Experimentalis. 2010; 58:107–19. [PubMed: 20143172]

Evans RK, Nawrocki DK, Isopi LA, Williams DM, Casimiro DR, Chin S, Chen M, Zhu D-M, Shiver JW, Volkin DB. Development of stable liquid formulations for adenovirus-based vaccines. Journal of Pharmaceutical Sciences. 2004; 93:2458–75. [PubMed: 15349956]

Faulkner RL, Jang M-H, Liu X-B, Duan X, Sailor KA, Kim JY, Ge S, Jones EG, Ming G-l, Song H, Cheng H-J. Development of hippocampal mossy fiber synaptic outputs by new neurons in the adult brain. Proceedings of the National Academy of Sciences. 2008; 105:14157–62.

Geddes BJ, Harding TC, Hughes DS, Byrnes AP, Lightman SL, Conde G, Uney JB. Persistent transgene expression in the hypothalamus following stereotaxic delivery of a recombinant adenovirus: suppression of the immune response with cyclosporin. Endocrinology. 1996; 137:5166–9. [PubMed: 8895393]

Geddes BJ, Harding TC, Lightman SL, Uney JB. Long-term gene therapy in the CNS: Reversal of hypothalamic diabetes insipidus in the Brattleboro rat by using an adenovirus expressing arginine vasopressin. Nature Medicine. 1997; 3:1402–4.

Ghirardello S, Garre M-L, Rossi A, Maghnie M. The diagnosis of children with central diabetes insipidus. Journal of Pediatric Endocrinology and Metabolism. 2007; 20:359–75. [PubMed: 17451074]

Harrison SC. Viral membrane fusion. Nat Struct Mol Biol. 2008; 15:690–8. [PubMed: 18596815]

Heger S, Mastronardi C, Dissen GA, Lomniczi A, Cabrera R, Roth CL, Jung H, Galimi F, Sippell W, Ojeda SR. Enhanced at puberty 1 (EAP1) is a new transcriptional regulator of the female neuroendocrine reproductive axis. The Journal of Clinical Investigation. 2007; 117:2145–54. [PubMed: 17627301]

NIH-PA Author Manuscript

NIH-PA Author Manuscript

NIH-PA Author Manuscript

Howarth J, Lee Y, Uney J. Using viral vectors as gene transfer tools (Cell Biology and Toxicology Special Issue: ETCS-UK 1 day meeting on genetic manipulation of cells). Cell Biology and Toxicology. 2009; 26:1–20. [PubMed: 19830583]

Ideno J, Mizukami H, Honda K, Okada T, Hanazono Y, Kume A, Saito T, Ishibashi S, Ozawa K. Persistent Phenotypic Correction of Central Diabetes Insipidus Using Adeno-associated Virus Vector Expressing Arginine-Vasopressin in Brattleboro Rats. Mol Ther. 2003; 8:895–902. [PubMed: 14664791]

Ivell R, Burback PH, Leeuwen FWV. The molecular biology of the Brattleboro rat. Frontiers in Neuroendocrinology. 1990; 4:313–38.

Klein RL, Dayton RD, Tatom JB, Henderson KM, Henning PP. AAV8, 9, Rh10, Rh43 Vector Gene Transfer in the Rat Brain: Effects of Serotype, Promoter and Purification Method. Mol Ther. 2007; 16:89–96. [PubMed: 17955025]

Klein RL, Hamby ME, Gong Y, Hirko AC, Wang S, Hughes JA, King MA, Meyer EM. Dose and Promoter Effects of Adeno-Associated Viral Vector for Green Fluorescent Protein Expression in the Rat Brain. Experimental Neurology. 2002; 176:66–74. [PubMed: 12093083]

Le Gal La Salle G, Robert JJ, Berrard S, Ridoux V, Stratford-Perricaudet LD, Perricaudet M, Mallet J. An adenovirus vector for gene-transfer into neurons and glia in the brain. Science. 1993; 259:988–90. [PubMed: 8382374]

Li M, Husic N, Lin Y, Christensen H, Malik I, McIver S, Daniels CML, Harris DA, Kotzbauer PT, Goldberg MP, Snider BJ. Optimal promoter usage for lentiviral vector-mediated transduction of cultured central nervous system cells. Journal of Neuroscience Methods. 2010; 189:56–64. [PubMed: 20347873]

Loeb JE, Cordier WS, Harris ME, Weitzman MD, Hope TJ. Enhanced Expression of Transgenes from Adeno-Associated Virus Vectors with the Woodchuck Hepatitis Virus Posttranscriptional Regulatory Element: Implications for Gene Therapy. Human Gene Therapy. 1999; 10:2295–305. [PubMed: 10515449]

Ma X-M, Wang Y, Ferraro F, Mains RE, Eipper BA. Kalirin-7 Is an Essential Component of both Shaft and Spine Excitatory Synapses in Hippocampal Interneurons. J Neurosci. 2008; 28:711–24. [PubMed: 18199770]

Mason MRJ, Ehlert EME, Eggers R, Pool CW, Hermening S, Huseinovic A, Timmermans E, Blits B, Verhaagen J. Comparison of AAV Serotypes for Gene Delivery to Dorsal Root Ganglion Neurons. Mol Ther. 2010; 18:715–24. [PubMed: 20179682]

Mastromarino P, Conti C, Goldoni P, Hauttecoeur B, Orsi N. Characterization of Membrane Components of the Erythrocyte Involved in Vesicular Stomatitis Virus Attachment and Fusion at Acidic pH. J Gen Virol. 1987; 68:2359–69. [PubMed: 2821175]

Meunier A, Pohl M. Lentiviral vectors for gene transfer into the spinal cord glial cells. Gene Ther. 2009; 16:476–82. [PubMed: 19242525]

Pasquale GD, Davidson BL, Stein CS, Martins I, Scudiero D, Monks A, Chiorini JA. Identification of PDGFR as a receptor for AAV-5 transduction. Nat Med. 2003; 9:1306–12. [PubMed: 14502277]

Paterna J, Feldon J, Bueler H. Transduction Profiles of Recombinant Adeno-Associated Virus Vectors Derived from Serotypes 2 and 5 in the Nigrostriatal System of Rats. J Virol. 2004; 78:6808–17. [PubMed: 15194756]

Persson A, Fan X, Salford LG, Widegren B, Englund E. Neuroblastomas and medulloblastomas exhibit more Coxsackie adenovirus receptor expression than gliomas and other brain tumors. Neuropathology. 2007; 27:233–6. [PubMed: 17645237]

Puntel, M.; Kroeger, KM.; Sanderson, NS.; Thomas, CE.; Castro, MG.; Lowenstein, PR. Gene Transfer into Rat Brain Using Adenoviral Vectors. John Wiley & Sons, Inc; 2010.

Qing K, Mah C, Hansen J, Zhou S, Dwarki V, Srivastava A. Human fibroblast growth factor receptor 1 is a co-receptor for infection by adeno-associated virus 2. Nat Med. 1999; 5:71–7. [PubMed: 9883842]

Rajani RR, Ball CG, Feliciano DV, Vercruysse GA. Vasopressin in Hemorrhagic Shock: Review Article. The American Surgeon. 2009; 75:1207–12. [PubMed: 19999914]

NIH-PA Author Manuscript

NIH-PA Author Manuscript

NIH-PA Author Manuscript

Reimsnider S, Manfredsson FP, Muzyczka N, Mandel Ronald J. Time Course of Transgene Expression After Intrastriatal Pseudotyped rAAV2/1, rAAV2/2, rAAV2/5, and rAAV2/8 Transduction in the Rat. Mol Ther. 2007; 15:1504–11. [PubMed: 17565350]

Rhodes CH, Morriell JI, Pfaff DW. Immunohistochemical analysis of magnocellular elements in rat hypothalamus: Distribution and numbers of cells containing neurophysin, oxytocin, and vasopressin. The Journal of Comparative Neurology. 1981; 198:45–64. [PubMed: 7014660]

Rosner M. Hyponatremia in Heart Failure: The Role of Arginine Vasopressin and Diuretics. Cardiovascular Drugs and Therapy. 2009; 23:307–15. [PubMed: 19554441]

Schaack J, Bennett ML, Shapiro GS, DeGregori J, McManaman JL, Moorhead JW. Strong foreign promoters contribute to innate inflammatory responses induced by adenovirus transducing vectors. Virology. 2011 In Press.

Schmale H, Richter D. Single base deletion in the vasopressin gene is the cause of diabetes insipidus in Brattleboro rats. Nature. 1984; 308:705–9. [PubMed: 6717565]

Sharman G, Ghorbel M, Leroux M, Beaucourt S, Wong L-F, Murphy D. Deciphering the mechanisms of homeostatic plasticity in the hypothalamo-neurohypophyseal system--genomic and gene transfer strategies. Progress in Biophysics and Molecular Biology. 2004; 84:151–82. [PubMed: 14769434]

Sherlock M, Thompson CJ. The syndrome of inappropriate antidiuretic hormone: current and future management options. Eur J Endocrinol. 2010; 162:S13–8. [PubMed: 20164215]

Shughrue PJ, Merchenthaler I. Distribution of estrogen receptor β immunoreactivity in the rat central nervous system. The Journal of Comparative Neurology. 2001; 436:64–81. [PubMed: 11413547]

Sinnayah P, Lindley TE, Staber PD, Cassell MD, Davidson BL, Davisson RL. Selective Gene Transfer to Key Cardiovascular Regions of the Brain: Comparison of Two Viral Vector Systems. Hypertension. 2002; 39:603–8. [PubMed: 11882616]

Sinnayah P, Lindley TE, Staber PD, Davidson BL, Cassell MD, Davisson RL. Targeted viral delivery of Cre recombinase induces conditional gene deletion in cardiovascular circuits of the mouse brain. Physiol Genomics. 2004; 18:25–32. [PubMed: 15069166]

Sladek, CD. Antidiuretic hormone: synthesis and release. In: Fray, JCS., editor. Handbook of Physiology. Oxford University Press; Oxford: 2000. p. 436-95.

Summerford C, Bartlett JS, Samulski RJ. $\alpha_V\beta_5$ integrin: a co-receptor for adeno-associated virus type 2 infection. Nat Med. 1999; 5:78–82. [PubMed: 9883843]

Summerford C, Samulski RJ. Membrane-Associated Heparan Sulfate Proteoglycan Is a Receptor for Adeno-Associated Virus Type 2 Virions. J Virol. 1998; 72:1438–45. [PubMed: 9445046]

Swanson LW, Sawchenko PE. Hypothalamic Integration: Organization of the Paraventricular and Supraoptic Nuclei. Annual Review of Neuroscience. 1983; 6:269–324.

Vasquez EC, Beltz TG, Haskell RE, Johnson RF, Meyrelles SS, Davidson BL, Johnson AK. Adenovirus-Mediated Gene Delivery to Cells of the Magnocellular Hypothalamo-neurohypophyseal System. Experimental Neurology. 2001; 167:260–71. [PubMed: 11161614]

Venkatraman G, Behrens M, Pyrski M, Margolis F. Expression of Coxsackie-Adenovirus receptor (CAR) in the developing mouse olfactory system. Journal of Neurocytology. 2005; 34:295–305. [PubMed: 16841169]

Xu L, Daly T, Gao C, Flotte TR, Song S, Byrne BJ, Sands MS, Ponder KP. CMV-β-Actin Promoter Directs Higher Expression from an Adeno-Associated Viral Vector in the Liver than the Cytomegalovirus or Elongation Factor 1α Promoter and Results in Therapeutic Levels of Human Factor X in Mice. Human Gene Therapy. 2001a; 12:563–73. [PubMed: 11268288]

Xu R, Janson CG, Mastakov M, Lawlor PA, Young D, Mouravlev AI, Fitzsimons HL, Choi H, Ma M, Dragunow M, Leone P, Chen Q, Dicker B, During MJ. Quantitative comparison of expression with adeno-associated virus (AAV-2) brain-specific gene cassettes. Gene Ther. 2001b; 8:1323–32. [PubMed: 11571569]

Zolotukhin S, Byrne BJ, Mason E, Zolotukhin I, Potter M, Chesnut K, Summerford C, Samulski RJ, Muzyczka N. Recombinant adeno-associated virus purification using novel methods improves infectious titer and yield. Gene Therapy. 1999; 6:973–85. [PubMed: 10455399]

NIH-PA Author Manuscript
NIH-PA Author Manuscript
NIH-PA Author Manuscript

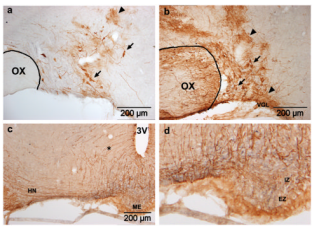

Figure 1. Adenoviral transduction in the SON

GFP expression four days after SON injection of Ad-GFP. Two titers were tested: (a) 6.7×10^{7} pfu in 0.6µl or (b,c) 1.1×10^{9} pfu in 1.0µl. In both cases, transduced neurons (arrows) and glia (arrowheads) are present. Astrocytes in the VGL below the SON are also transduced (b). Stained fibers in the HN (c) and internal zone of the ME (d) confirm the presence of transduced SON MNCs. Stained tanycytes and their fibers (asterisk) are also visible (c). OX, optic chiasm; 3V, third ventricle; VGL, ventral glial lamina; ME, median eminence; HN, hypthalamo-neurohypophyseal tract; IZ, internal zone; EZ, external zone.

NIH-PA Author Manuscript

NIH-PA Author Manuscript

NIH-PA Author Manuscript

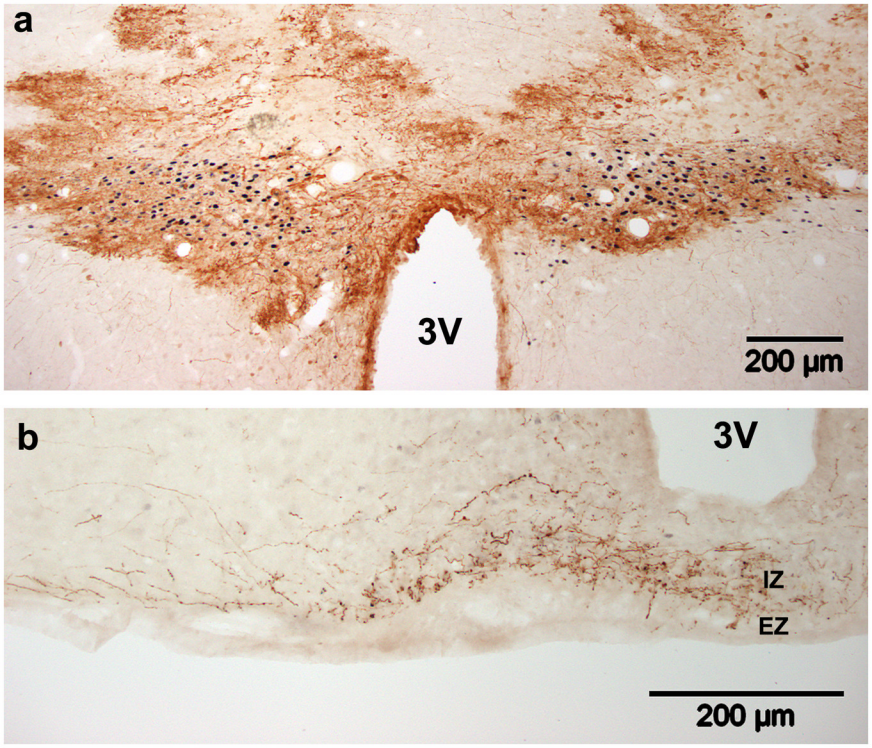

Figure 2. Adenovirus transduction in the PVN

GFP expression seven days after bilateral injection of Ad-GFP (3.0×10^6 pfu in 0.3μl) just above the PVN. (a) GFP expression (brown) in the PVN (delineated by black nuclear ERβ staining). (b) Though dense staining in the PVN prevents identification of affected cell types, fibers in the internal zone of the median eminence (ME) confirm transduction of MNC neurons, while fibers in the external zone indicate transduction of parvocellular neurons. 3V, third ventricle; IZ, internal zone; EZ, external zone.

NIH-PA Author Manuscript
NIH-PA Author Manuscript
NIH-PA Author Manuscript

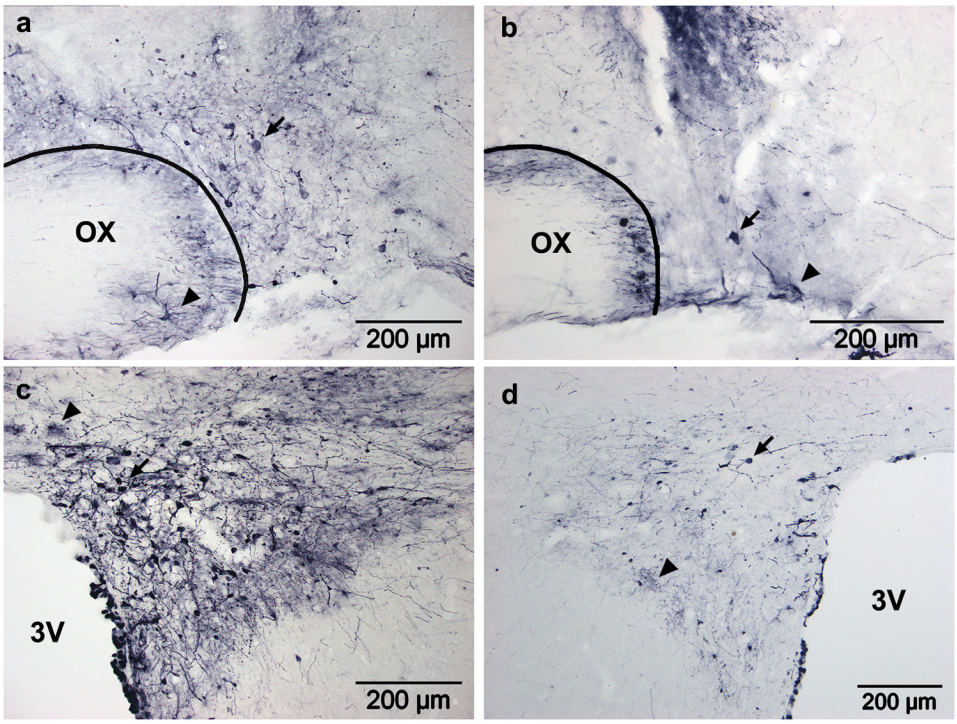

Figure 3. Timecourse of GFP expression in SON and PVN after Ad-GFP injection

GFP expression in transduced cells is dramatically decreased by 4 weeks post-injection in both nuclei. (a,b) GFP expression in the SON and (c,d) PVN. (a,c) Two and (b,d) four weeks post injection. Transduced neurons (arrows) and glia (arrowheads) are present. OX, optic chiasm; 3V, third ventricle.

NIH-PA Author Manuscript
NIH-PA Author Manuscript
NIH-PA Author Manuscript

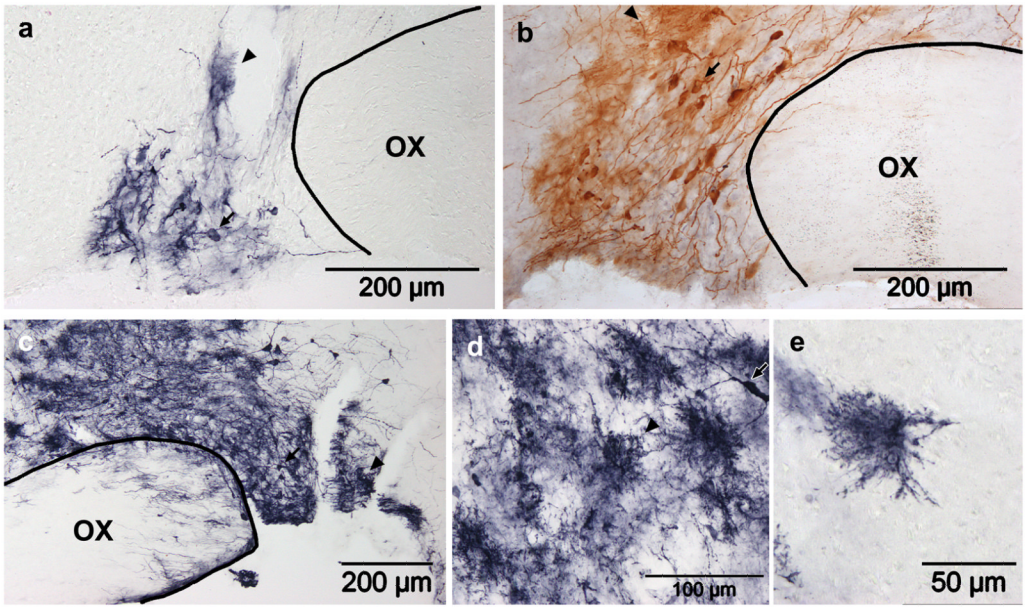

Figure 4. Lentiviral (HIV-GFP) transduction in the SON

(a) GFP expression four and (b–e) eight days after HIV-GFP injection. Two titers were tested: (a,b) 5.0×10^5 TU in 1.0µl or (c–e) 2.25×10^6 TU in 2.5µl. In all cases, transduced neurons (arrows) and glia (arrowheads) are present. High magnification reveals that the glia in the injection track (d) and isolated glia nearby (e) morphologically resemble protoplasmic glia. The conventional immunoperoxidase reaction results in brown staining (b), while a nickel-enhanced reaction results in dark purple staining (a,c,d,e). OX, optic chiasm.

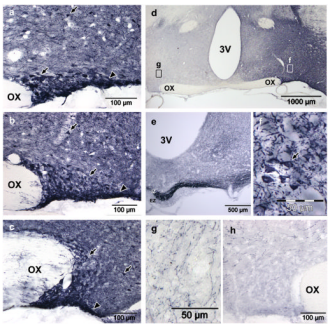

Figure 5. AAV2-CAG-GFP transduction in the SON four weeks after injection using convection enhanced delivery

(a–c) GFP expression was very high in the anterior (a), mid (b) and posterior (c) SON after rapid injection (0.25µl/min) of 3.25×10^{9}gp in 2.5µl. Arrows indicate neurons within or outside of the SON; arrowheads indicate the location of the ventral glial lamina. (d) A low power view of the hypothalamus shows that the dark staining is specific and restricted to the injected side. Fields of view for (f) and (g) are indicated. (e) Dense staining in the median eminence indicates efficient transduction of MNCs, though very dark staining in the SON is too dark to accurately count cells. Dark staining in the ipsilateral hypothalamus (a–d) is the result of a dense web GFP filled neurons and neurites (f). The contralateral hypothalamus also shows far fewer stained neurites and no cell bodies (g). Despite the large volume injected, the vector did not spread beyond the ipsilateral hypothalamus and, the contralateral hypothalamus (g) and SON (h) did not contain any GFP positive soma. OX, optic chiasm; 3V, third ventricle; IZ, internal zone; EZ, external zone.

NIH-PA Author Manuscript NIH-PA Author Manuscript NIH-PA Author Manuscript

NIH-PA Author Manuscript
NIH-PA Author Manuscript
NIH-PA Author Manuscript

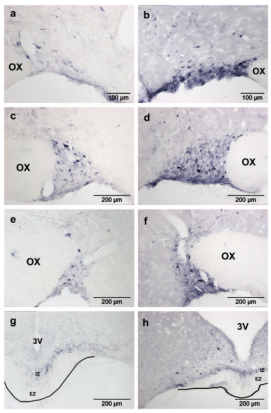

Figure 6. AAV5-GFP transduction in the SON after injection using convection enhanced delivery

The number of GFP positive MNCs increased dramatically between three (a,c,e,g) and four (b,d,f,h) weeks post injection. At both timepoints, GFP positive MNCs were prominent in the anterior (a,b), mid (c,d) and posterior (e,f) SON, and there was no evidence of transduced glia. MNC axons are visible in the internal zone of the median eminence (g,h), and their sparseness is likely due to low GFP expression in neurites. OX, optic chiasm; 3V, third ventricle; IZ, internal zone; EZ, external zone.

NIH-PA Author Manuscript

NIH-PA Author Manuscript

NIH-PA Author Manuscript

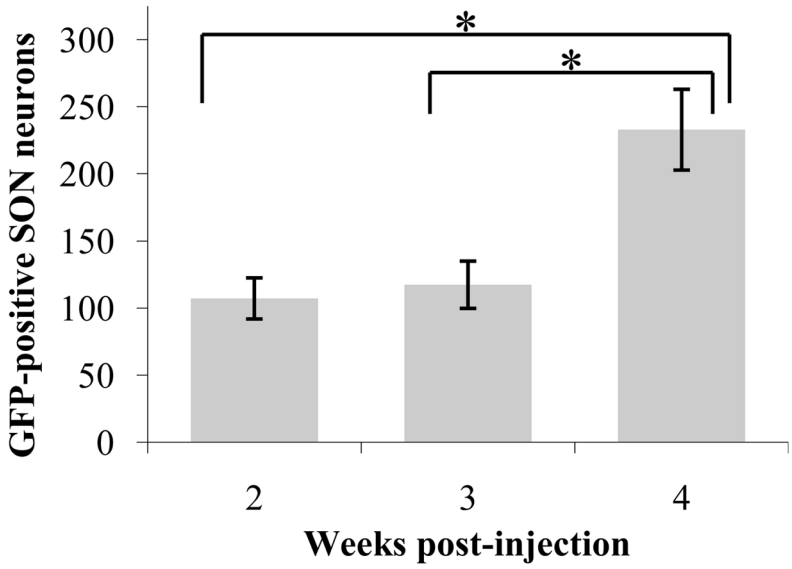

Figure 7. Timecourse of GFP expression after AAV5 injection

The number of GFP-positive neurons per injected SON increases dramatically between three and four weeks post-injection. *p<0.05

NIH-PA Author Manuscript
NIH-PA Author Manuscript
NIH-PA Author Manuscript

Table 1

Injection details by vector

	Ad-GFP	Ad-GFP	HIV-GFP	AAV2/5-EGFP	AAV2-GFP
Nucleus injected	SON	PVN	SON	SON	SON
Injection coordinates (mm from bregma)	p1.1, l1.4, v8.7[a]	10° toward midline p2.0, l1.7, v7.6[a]	p1.2, l1.4, v9.2[a]	p1.1, l1.7, v8.9[a]	p1.1, l1.7, v8.9[a]
Viral titer	1.1×10^{11} or 1.1×10^{12} pfu[b]/ml	1.0×10^{10} pfu[b]/ml	5.0×10^{8} TU[c]/ml	1.1×10^{12} GC[d]/ml	1.3×10^{12} gp[e]/ml
Volume injected	0.6 or 1.0 μl	0.3 or 0.5 μl	1.0 or 2.5 μl	2.5 μl	2.5 μl
Total virus injected	6.7×10^{7},1.1×10^{8} or 1.1×10^{9} pfu[b]	3.0×10^{6} or 1.0×10^{7} pfu[b]	5.0×10^{5} or 2.25×10^{6} TU[c]	2.75×10^{9} GC[d]	3.25×10^{9} gp[e]
Times tested	4–28 days	7–28 days	4–8 days	14–28 days	28 days

[a] p, posterior; l, lateral; v, ventral

[b] pfu, plaque forming units

[c] TU transducing units

[d] GC, genomic copies

[e] gp, genomic particles

NIH-PA Author Manuscript

NIH-PA Author Manuscript

NIH-PA Author Manuscript

Table 2

Comparison of viral vector characteristics

	Adenovirus	Lentivirus	Adeno-associated virus
Vector particle size	70–90 nm[e]	80–120 nm[c]	18–26 nm[e]
Genome size	~ 36 Kb[e]	~ 10 Kb[e]	~ 5 Kb[e]
Space for cloned sequence	~ 8 Kb[e]	~ 10 Kb[c]	~ 5 Kb[e]
Genome structure	Linear dsDNA[e]	Linear ssRNA, + only[c]	Linear ssDNA, + or −[e]
Envelope	None[e]	VSVG glycoprotein[c]	None[e]
Latency to peak transgene expression	3–5 days[i,k]	~7 days[j]	~2–4 weeks[e]
Rate limiting step before expression	DNA into nucleus[e]	Integration into host genome[e]	Second strand synthesis[e]
Can integrate into host genome?	No, but in nucleus[e]	Yes, non-specific[e]	Yes, inefficient[e]
Expression requires integration?	No[e]	Yes[e]	No[e]
Inflammatory?	Yes[i]	No[e]	No[e]
Duration of transgene expression	Weeks/months[e,i]	Years[e]	Years[e]
Transduces post-mitotic cells?	Yes[e]	Yes[c]	Yes[e]
Neuronal transduction	Moderate[i,j]	Moderate[a,d]	Very strong [b,f,h]
Glial transduction	Strong[i,j]	Moderate[a,g]	Very minimal or none[b,f,h]

[a] Blits et al., 2010

[b] Burger et al., 2004

[c] Escors and Breckpot, 2010

[d] Heger et al., 2007

[e] Howarth et al., 2009

[f] Mason et al., 2010

[g] Meunier and Pohl, 2009

[h] Paterna et al., 2004

[i] Puntel et al., 2010

[j] Sinnayah et al., 2002

[k] Vasquez et al., 2001